

Multi-physics Simulation of Non-linear Opto-Mechanical Coupling in Micro-structured resonant cavities

Matteo Stocchi*, Davide Mencarelli*[†] and Luca Pierantoni*[†]

*Università Politecnica delle Marche, Ancona, 60131, Italy

[†]Istituto Nazionale di Fisica Nucleare (INFN) - Laboratori Nazionali di Frascati (LNF), Via E. Fermi, Frascati, Roma (Italy)

Abstract—The application described in this paper was presented as part of the Student Design Competitions at the 2017 IEEE Microwave Theory and Techniques Society (MTT-S) International Microwave Symposium (IMS). The objective of our particular branch of the aforementioned competition, sponsored by the MTT-25 technical committee on RF-Nanotechnology, was to develop an application for hand-held devices or personal computers that could not only support instruction in the principles and uses of electromagnetic theory as related to RF nanotechnologies, but also be applied to solve specific design problems. In what follows, an application capable of accurately predicting the behaviour of an opto-mechanical environment will be introduced, giving particular emphasis to the implementation of the various bridging terms related to the coupled physics, i.e. the electrodynamics and the continuum mechanics. In order to provide an illustrative example, an original opto-mechanical cavity has been designed, to evaluate the efficiency of the phenomenon under investigation.

I. INTRODUCTION

The interfacing between optical cavities and mechanical systems has given rise to a rapid development of cavity optomechanics, which aims to confine light into small volumes, by the means of an high-Q resonant recirculation [1], [2]. The purpose of an optomechanical system is to investigate the interaction of light with a mechanical oscillator, and its highly interdisciplinary nature leads to several potential applications in various fields of research, especially in quantum processing. Although electromagnetic radiation has historically been the primary experimental tool for controlling a quantum system and for transmitting and distributing quantum information, there is a growing interest in using acoustic or mechanical waves for inspecting quantum control and on-chip quantum communication of artificial atoms. Recently, experimental and theoretical analyses have included coherent coupling of Surface Acoustic Waves (SAWs) or mechanical vibrations to superconducting qubits [3], SAW-based universal quantum transducers [4], mechanical quantum control of electron spins in diamond [5], phononic QED [6] and phonon-mediated spin squeezing [7]. The most successful exploitation of mechanical vibrations for quantum control, however, combines both optical and mechanical interactions through phonon-assisted optical or sideband transitions, as demonstrated in trapped ions [8], [9] and, more recently, in cavity optomechanics [10], [11]. Focusing on the latter, optomechanical micro-cavities can also provide new functionalities, applications and opportunities, beyond standard technology, owing to phonon

propagation, generation, and processing [12]. Such an application would require low power consumption and, making a comparison with pure nano electromechanical actuation, the optical approach ensures fewer impedance mismatch issues. Additionally, phonons are an excellent interface to coherently transfer information, for instance, between microwaves and optical photons, between magnons and photons, etc. In this contribution, we present a fully-coupled numerical approach which accurately predicts the optomechanical dynamics in microstructured resonant cavities. The rigorousness of the analysis is ensured by considering all the energy-transduction contributes [13], summarized in *Fig. 1*. Radiation pressure and electrostriction constitute the forces exerted by the electromagnetic fields on matter, whereas the photoelasticity describes the perturbation of the electromagnetic radiation caused by the presence of the mechanical wave. Special considerations are required for the so called *moving boundary* effect, i.e. the boundary deformation caused by the space-time-varying pressure field that perturbs the electromagnetic boundary conditions. Specifically, the Eulerian coordinates in which the Maxwell equations are solved are not able to take into account mechanical displacement, defined, in turn, in Lagrangian coordinates. This limitation can be numerically significant in case of micro- and nano-scale cavities. The Transformation Optics (TO) [14], [15] method represents an elegant and efficient solution to the just addressed problem. TO is a relatively recent technique that can facilitate the design of a variety of optical devices (lenses, phase shifters, deflectors, etc.) by deforming the coordinate system, warping space to control the trajectories of the electromagnetic radiation. Such alteration then turns into a change of the electromagnetic material parameters such as the permittivity ϵ and the permeability μ . For the special case of optomechanics, in the next section, TO is used to take into account the time-varying boundaries of the domain under investigation [16], making it possible to consider the moving boundary effect by the mean of a modified version of the standard Helmholtz equation.

II. THEORETICAL FOUNDATIONS

Optomechanics arises from the combination between continuum mechanical physics, a branch of mechanics that studies the mechanical behaviour of materials modelled as a continuous mass rather than as discrete particles, and classic electrodynamics, governed by Maxwell equations. The

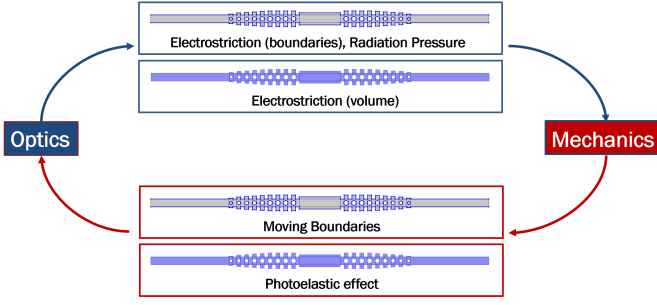


Fig. 1: Sketch of the four coupling contributes of an optomechanical interaction.

foundations of the phenomenon rely on the relation [17]

$$\omega_1 = \Omega + \omega_2, \quad (1)$$

where Ω is the mechanical frequency and $\omega_{1,2}$ are the optical ones, respectively of the pumped and of the scattered light. Eq. (1) states the exchange of energy between electromagnetic radiation and the mechanical motion, also defining the matching condition for the time-dependent source terms that enter in the ruling equations of the physics of interest. A general mechanical wave, whether it is confined in a mechanical cavity or free to propagate, is efficiently described in terms of the displacement \mathbf{u} , i.e. the deformation of a considered elementary cell of the medium under investigation with respect to the relaxation point. The displacement \mathbf{u} satisfies the conservation law of the linear momentum [18]

$$\rho_0 \Omega^2 \mathbf{u} + \nabla_{\mathbf{x}} \cdot (\overline{\overline{\mathbf{F}\mathbf{S}}}) = -\mathbf{F}_{RP} - \mathbf{F}_{ES,V} - \mathbf{F}_{ES,B}, \quad (2)$$

where ρ_0 the mass density of the undeformed configuration, $\overline{\overline{\mathbf{F}}}$ the deformation gradient tensor, $\overline{\overline{\mathbf{S}}}$ the second Piola-Kirchhoff tensor and $\nabla_{\mathbf{x}}$ indicates the nabla operator expressed in Lagrangian coordinates. The right-side of eq. (2) introduces two of the four aforementioned coupling parameters of an optomechanical phenomenon, i.e. the electrostriction and the radiation pressure forces. The electrostriction is the tendency of materials to become compressed in the presence of an E-field. From a microscopic point of view, the electrostrictive force acting on the molecule is given by

$$\mathbf{F}_{ES} = -\nabla U = \frac{1}{2} \epsilon_0 \alpha \nabla (E^2), \quad (3)$$

where α is the molecular polarizability. As it can be easily noticed, the force \mathbf{F}_{ES} tends to push the molecule to the region where the E-field is stronger. For numerical purposes is convenient to split the electrostrictive force in two separate contributes, the electrostrictive force acting on the whole volume of the considered body and the electrostrictive force acting only on the boundaries of it. Accounting then also for the radiation pressure forces, the three terms on the right-side

of eq. (2) can be written as [19]

$$\mathbf{F}_{ES,V} = f_x^{ES,V} \hat{x} + f_y^{ES,V} \hat{y} + f_z^{ES,V} \hat{z}, \quad (4)$$

$$\mathbf{F}_{ES,B} = (\sigma_{1ij} - \sigma_{2ij}) n_j, \quad (5)$$

$$\mathbf{F}_{RP} = -\frac{1}{2} \epsilon_0 E_{t,1} E_{t,2}^* (\epsilon_2 - \epsilon_1) \mathbf{n} + \frac{1}{2} \epsilon_0^{-1} D_{1,n}^2 (\epsilon_2^{-1} - \epsilon_1^{-1}) \mathbf{n}, \quad (6)$$

where the individual force components appearing in eq. (4) are given by

$$f_x^{ES,V} = -\partial_x \sigma_{xx} - \partial_y \sigma_{xy} - \partial_z \sigma_{xz}, \quad (7)$$

$$f_y^{ES,V} = -\partial_x \sigma_{xy} - \partial_y \sigma_{yy} - \partial_z \sigma_{yz}, \quad (8)$$

$$f_z^{ES,V} = -\partial_x \sigma_{xz} - \partial_y \sigma_{yz} - \partial_z \sigma_{zz}, \quad (9)$$

and the components of the so called electrostrictive tensor $\overline{\overline{\sigma}}$ are defined as

$$\sigma_{ij} = -\frac{1}{2} \epsilon^2 p_{ijkl} E_k E_l, \quad (10)$$

in which we find the strain-optic tensor p_{ijkl} . Two additional mechanical quantities are now introduced: the effective mass m_{eff} and the thermally-caused initial displacement u_0 . For a non-ideal oscillating system, an effective mass m_{eff} has to be considered, so that is possible to study the latter as a simple harmonic oscillator. For any resonating mode of a mechanical oscillator, a numerical estimation of the effective mass is given by [20]

$$m_{eff} = \int \rho_0 |\mathbf{u}|^2 dV, \quad (11)$$

where the displacement \mathbf{u} is made dimensionless by normalizing it over its maximum value. At a given temperature T the phonon occupation related to a particular resonant mechanical mode can be estimated, in terms of an initial displacement u_0 , as [21]

$$u_0 = \frac{4k_B T}{m_{eff} \Omega^2}. \quad (12)$$

The effective mass m_{eff} and the resonant mode frequency Ω clearly define the entity of the initial displacement u_0 : the lower they are, the larger is the thermal displacement. For the general case of an anisotropic and inhomogeneous medium, the electromagnetic field can be efficiently described, as usual, by means of the Helmholtz equation

$$\nabla^2 \mathbf{E}_1 = -\mu \omega_1^2 \mathbf{P}_1 = \frac{\mu \omega_1^2}{2} \sum_{kl} \epsilon_{ij}^2 p_{ijkl} \epsilon_{kl} \mathbf{E}_2, \quad (13)$$

$$\nabla^2 \mathbf{E}_2 = -\mu \omega_2^2 \mathbf{P}_2 = \frac{\mu \omega_2^2}{2} \sum_{kl} \epsilon_{ij}^2 p_{ijkl}^* \epsilon_{kl}^* \mathbf{E}_1, \quad (14)$$

opportunately split in its two harmonic components of interest $\omega_{1,2}$. The term on the right-hand side of eq.s (13,14) introduces the mechanical perturbation due to the photoelastic effect, represented by the strain tensor ε_{kl} . Further investigations are needed in order to take into account for the second mechanical contribute to the electromagnetic field, i.e. the moving boundary effect. In the full-wave simulator, Maxwell equations are solved in Eulerian coordinates, that are not automatically able to account the effect of the displacement on the boundaries. Transmission Optics (TO) offers a valid solution to overcome such a problem. In fact, by considering the general formulation of the TO method, we have

$$\bar{\bar{\epsilon}}' = \frac{\bar{\bar{A}\bar{A}}}{\det \bar{\bar{A}}} \bar{\bar{\epsilon}}, \quad (15)$$

$$\bar{\bar{\mu}}' = \frac{\bar{\bar{A}\bar{A}}}{\det \bar{\bar{A}}} \bar{\bar{\mu}}, \quad (16)$$

where $\bar{\bar{A}}$ is the Jacobian related to the desired coordinate transformation, the proposed procedure [16] replaces the latter with the before introduced deformation gradient $\bar{\bar{F}}$, leading to

$$\bar{\bar{\epsilon}}' = \frac{\bar{\bar{F}\bar{F}}}{\det \bar{\bar{F}}} \bar{\bar{\epsilon}} = \bar{\bar{g}} \bar{\bar{\epsilon}}, \quad (17)$$

$$\bar{\bar{\mu}}' = \frac{\bar{\bar{F}\bar{F}}}{\det \bar{\bar{F}}} \bar{\bar{\mu}} = \bar{\bar{g}} \bar{\bar{\mu}}, \quad (18)$$

where we defined $\bar{\bar{g}}$ as the metric tensor, which is composed by terms having different harmonics

$$\bar{\bar{g}} = \sum_{n=-3}^3 \bar{\bar{g}}_n e^{in\Omega t}. \quad (19)$$

By eq. (15) and eq. (16), it is possible to take into account both the photoelasticity and the moving boundary effects in the Maxwell equations

$$-\nabla \times \tilde{\mathbf{E}} = \frac{\partial}{\partial t} (\bar{\bar{g}} \mu \tilde{\mathbf{H}}) \quad (20)$$

$$\nabla \times \tilde{\mathbf{H}} = \frac{\partial}{\partial t} [\bar{\bar{g}} (\bar{\bar{\epsilon}} + \epsilon_0 \bar{\Delta} \bar{\bar{\epsilon}}) \tilde{\mathbf{E}}] + \bar{\bar{g}} \sigma_e \tilde{\mathbf{E}}, \quad (21)$$

then, it is straightforward to derive the corresponding modified version of the Helmholtz equations for the considered harmonics

$$\begin{aligned} & \nabla \times \bar{\bar{A}}^{-1} \nabla \times \mathbf{E}_1 - \omega_1^2 \bar{\bar{C}} \mathbf{E}_1 = \\ & = \omega_1^2 [\bar{\bar{K}} \mathbf{E}_1 + (\bar{\bar{D}} + \bar{\bar{L}}) \mathbf{E}_2] - i\omega_1 \nabla \times (\bar{\bar{A}}^{-1} \bar{\bar{B}} \mathbf{H}_2) \end{aligned} \quad (22)$$

$$\begin{aligned} & \nabla \times \bar{\bar{A}}^{-1} \nabla \times \mathbf{E}_2 - \omega_2^2 \bar{\bar{C}} \mathbf{E}_2 = \\ & = \omega_2^2 [\bar{\bar{K}} \mathbf{E}_2 + (\bar{\bar{D}}^* + \bar{\bar{L}}^2) \mathbf{E}_1] - i\omega_2 \nabla \times (\bar{\bar{A}}^{-1} \bar{\bar{B}} \mathbf{H}_1) \end{aligned} \quad (23)$$

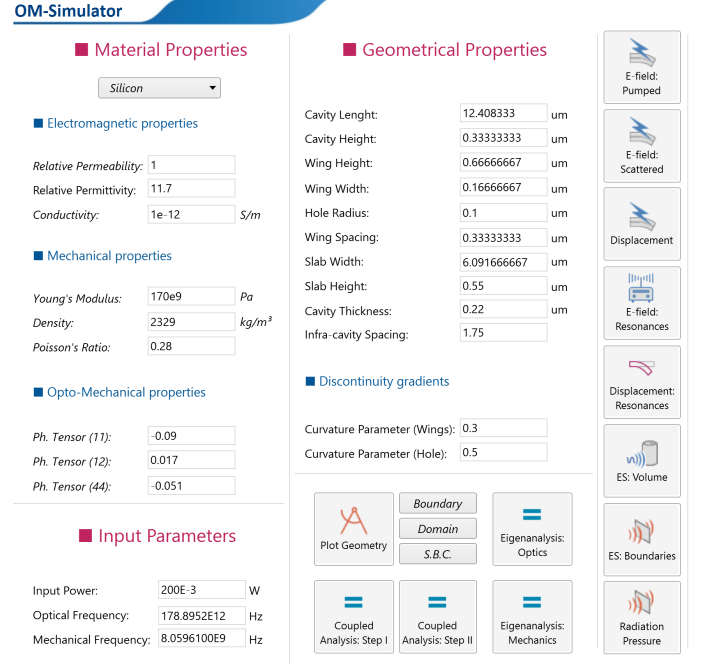


Fig. 2: Snapshot of the graphic user interface of the developed application. Four sections can be easily distinguished: The *Material Properties* section, in which it is possible to specify the physical characteristics of the sample taken into examination, the *Geometrical Properties* section, the *Input Parameters* section, in which frequencies (both optic and mechanical) and the laser input power are defined and the *Evaluation & Results* section.

in order to derive a more elegant form of the equation, we introduced the following second rank tensors:

$$\begin{aligned} \bar{\bar{A}} &= \bar{\bar{g}}_0 \mu, \\ \bar{\bar{B}} &= \bar{\bar{g}}_1 \mu, \\ \bar{\bar{C}} &= \bar{\bar{g}}_0 \epsilon, \\ \bar{\bar{D}} &= \bar{\bar{g}}_1 \epsilon, \\ \bar{\bar{K}} &= \frac{\epsilon_0}{2} (\bar{\bar{g}}_1 \bar{\Delta} \bar{\bar{\epsilon}}^* + \bar{\bar{g}}_1^* \bar{\Delta} \bar{\bar{\epsilon}}), \\ \bar{\bar{L}} &= \frac{\epsilon_0}{2} (\bar{\bar{g}}_2 \bar{\Delta} \bar{\bar{\epsilon}}^* + \bar{\bar{g}}_2^* \bar{\Delta} \bar{\bar{\epsilon}}). \end{aligned} \quad (24)$$

III. DESCRIPTION OF THE APPLICATION AND ITS GRAPHIC USER INTERFACE

The *Opto-Mechanical Cavities Simulator* application propose has been developed in COMSOLTMMultiphysics. As shown in Fig. 2, the graphic user interface can be split into four sections, each one related to a particular aspect of the design process:

- The *Material Properties* section incorporates all the electromagnetic (relative permeability ϵ_r , relative permittivity

μ_r and electrical conductivity σ_e), mechanical (Young's modulus E , mass density of the inderofmed configuration ρ_0 and Poisson's ratio ν) and opto-mechanical (photo-elastic tensor p_{ijkl}) parameters of the material the cavity is constituted from.

- The *Geometrical Parameters* section guides the user in designing and optimizing the desired opto-mechanical cavity. It is possible to engineer both the fundamental (cavity length and the cavity width) and the advanced (discontinuities and wings height curvature coefficients) geometrical parameters.
- The *Input Parameters* allows the user to define the desired frequencies, both optical and mechanical, relative to particular resonating modes and the input power P_{in} of the pumped laser.
- The *Evaluation & Results* section presents a list of sixteen buttons in total, conceptually divided into three categories: the geometry visualization buttons, the evaluation buttons and the result buttons. The geometry visualization buttons shows the geometrical entities which are relevant from a computational point of view, as the boundaries in which the surface forces (i.e. the radiation pressure and the boundary electrostrictive forces) are defined and the volume in which the opto-mechanical coupling takes place. The evaluation buttons allow the user to choose between three different studies: two eigenfrequency studies defined for both the electromagnetic and the mechanical modules, so that is possible to identify the various resonances of the resonant cavity under investigation, and one study which solves for the actual fully-coupled opto-mechanical phenomenon. The result buttons display the previously computed quantities of interest such as the fields distributions and the opto-mechanical coupling forces.

IV. EXAMPLES AND RESULTS

In this section we present an example in which the proposed application has been used in order to design an opto-mechanical cavity. The latter is composed of two optically coupled silicon-based cavities, with possibly different, geometry controlled, coupling rates. The degeneracy of the optical resonance of the individual cavities is broken by the mutual coupling, when the separation d between the cavities is reduced: for numerical purposes, different peak separations are considered, by just changing the parameter d (highlighted in Fig. 3). The corresponding frequency differences of the un-degenerate resonances are then obtained. The values of d are set by matching the above frequency difference with the resonant frequency of a specific mechanical mode, as stated in eq. (1). By considering a pumped power $P_{in} = 200$ mW, the optical and mechanical frequencies of the resonating modes are $f_1 = 178.89$ THz and $f_{mech} = 8.05$ GHz. The corresponding field distributions are shown in Fig. 4. The effective mass m_{eff} and the initial displacement u_0 associated to the chosen mechanical mode are, respectively, $1.44 \cdot 10^{-16}$ m and $2.09 \cdot 10^{-13}$ m. The reason why the

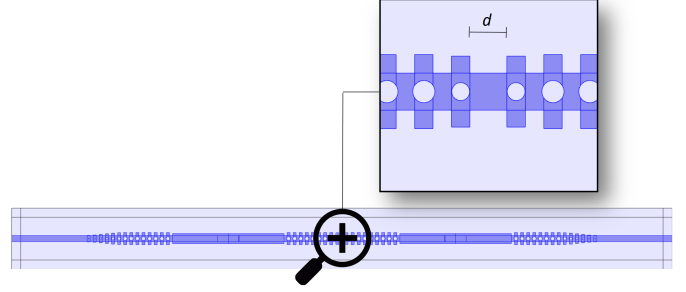


Fig. 3: Highlights of the parameters d , i.e. of the distance between the two coupled opto-mechanical cavities. The latter can be optimized in order to shift the two optical resonant modes related to the two frequencies ω_1 and ω_2 .

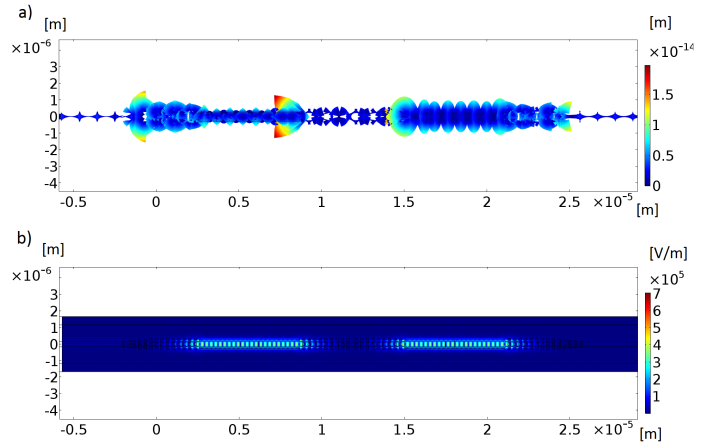


Fig. 4: Displacement field distribution of the enhanced mechanical resonating mode, with a mechanical isotropic loss factor of $\xi = 10^{-3}$ a), and norm of the E-field of the pumped optic resonant mode b). In the latter, the electromagnetic energy is well confined into the cavity, leading to high values of the optical Q-factor ($\sim 10^5$) and of the E-field itself.

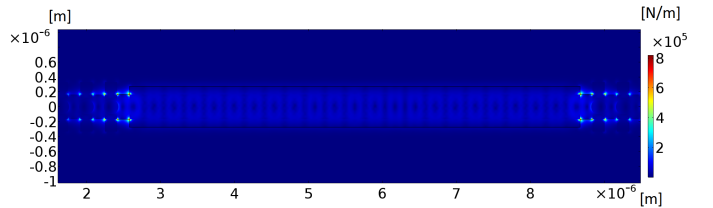


Fig. 5: Evaluation of the electrostrictive volume forces $\mathbf{F}_{ES,V}$ (N/m^3).

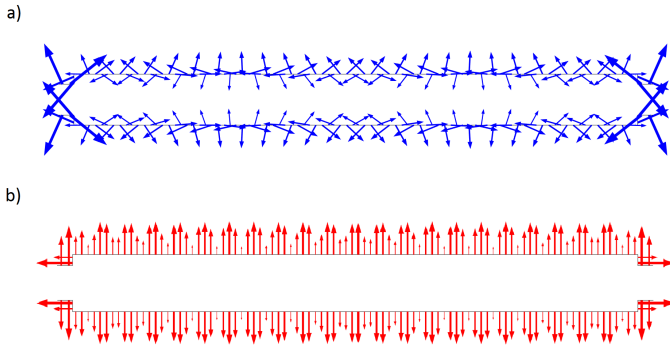


Fig. 6: Visualization of the boundary forces $\mathbf{F}_{ES,B}$ (Pa) a) and \mathbf{F}_{RP} (Pa) b) for the slab-like section of the optomechanical cavity. We can notice that the two coupling contributes, coming from different physical phenomenon, may also be opposite, leading to an attenuation of the overall coupling effect.

opto-mechanical coupling between the two resonant modes is quite high can be explained by just looking at the field distributions. Their confinement occurs in the same area of the opto-mechanical cavity, i.e. the two slab-like sections, that considerably enhances the coupling coefficients. The bulk force density $\mathbf{F}_{ES,V}$ is reported in Fig. 5, while the boundary forces $\mathbf{F}_{ES,B}$ and \mathbf{F}_{RP} are shown in Fig. 6. It is evident that the highest electrostrictive forces occurs in correspondence of abrupt discontinuities. It is also noted that the OM interaction cumulates over the whole length of the cavity.

V. CONCLUSIONS

A fully-coupled numerical approach that accurately predicts the opto-mechanical dynamics in micro- and nano-structured resonant cavities has been embedded in a COMSOLTM-based application. Based on an original-design for an opto-mechanical cavity, the quantities of interest such as the force-like coupling contributes $\mathbf{F}_{ES,V}$, $\mathbf{F}_{ES,B}$, \mathbf{F}_{RP} and the field distributions, both mechanical and optical, have been derived. As a progress of the theoretical platform, the 2D-model will be extended in a 3D environment. Moreover, a consistent version of the model will be provided for the full-wave analysis in the time-domain.

ACKNOWLEDGMENTS

This research is supported by the European Project All-Phononic circuits Enabled by Opto-mechanics PHENOMEN, H2020 FETOPEN 2014-2015-RIA, n.713450.

REFERENCES

- [1] M. Aspelmeyer, S.Gröblacher, K.Hammerer and N.Kiesel, "Quantum optomechanicsthrowing a glance," *J. Opt. Soc. Am.*, **B27**, pp. 189-197 , 2010.
- [2] F. Marquardt and S.M.Girvin, "Optomechanics (a brief review)," *arXiv:0905.0566*.
- [3] M.V.Gustafsson, T.Aref, A.F.Kockum, M.K.Ekstrom, G.Johansson and P. Delsing, "Propagating phonons coupled to an artificial atom," *Science*, vol. 346, no. 207, 2014.

- [4] M.J.A.Schuetz, E.M.Kessler, G.Giedke, L.M.K.Vandersypen, M.D.Lukin and J. I. Cirac, "Universal Quantum Transducers Based on Surface Acoustic Waves," *Physical Review X*, vol. 5, no. 031031, 2015.
- [5] E.R.MacQuarrie, T.A.Gosavi, N.R.Jungwirth, S.A.Bhave, and G.D.Fuchs, "Mechanical Spin Control of Nitrogen-Vacancy Centers in Diamond", *Physical Review Letters* , vol. 111, no. 227602, 2013.
- [6] O.O.Soykal, R.Ruskov, and C.Tahan, "Sound-Based Analogue of Cavity Quantum Electrodynamics in Silicon," *Physical Review Letters* , vol. 107, no. 235502, 2011.
- [7] S.D.Bennett, N.Y.Yao, J.Otterbach, P.Zoller, P.Rabl, and M.D.Lukin, "Phonon-Induced Spin-Spin Interactions in Diamond Nanostructures: Application to Spin Squeezing," *Physical Review Letters*, vol. 110, no. 156402, 2013.
- [8] D.Leibfried, R.Blatt, C.Monroe, and D.Wineland, "Quantum dynamics of single trapped ions," *Review of Modern Physics* , vol. 75, no. 281, 2003.
- [9] D.J.Wineland, "Nobel Lecture: Superposition, entanglement, and raising Schrodinger's cat," *Review of Modern Physics*, vol. 85, no. 1103, 2013.
- [10] M.Aspelmeyer, T.J.Kippenberg, and F.Marquardt, "Cavity optomechanics", *Reviews of Modern Physics*, vol. 86, no. 1391, 2014.
- [11] M.Metcalf, "Applications of cavity optomechanics", *Applied Physics Reviews*, vol. 1, no. 031105 , 2014.
- [12] K.Fang, M.H.Matheny, X.Luan and O.Painter, "Optical transduction and routing of microwave phonons in cavity-optomechanical circuits", *Nature Photonics*, vol. 10, pp. 489-496 , 2016.
- [13] C.Wol, M.J.Steel, B.J.Eggleton, and C.G.Poulton, "Stimulated Brillouin Scattering in integrated photonic waveguides: forces, scattering mechanisms and coupled mode analysis," *Physical Review A*, vol. 92, no. 013836 , 2015.
- [14] J.B.Pendry; D.Schurig.; D.R.Smith, "Controlling Electromagnetic Electromagnetic Fields," *Science*, vol. 312, no. 5514 , 2006.
- [15] D.Schurig, "Metamaterial Electromagnetic Cloak at Microwave Frequencies," *Science*, vol. 314, no. 5801 , 2006.
- [16] R.Zecca, P.T.Bowen, D.R.Smith, S.Larouche, "Transformation-optics simulation method for stimulated Brillouin scattering," *Phys. Rev. A*, vol. 94, no. 063818 , 2016.
- [17] R.W. Boyd, "Nonlinear optics," *Academic Press, 2008) Chap. 9, pp. 429, 3rd Ed.*
- [18] O.Gonzalez and A.M.Stuart, "A rst course in continuum mechanics," *(Cambridge University Press, 2008) Chap. 3, 5, pp. 94, 179193, 1st ed.*
- [19] W.Qiu, P.T.Rakich, H.Shin, H.Dong, M.Soljai and Z.Wang, "Stimulated Brillouin scattering in nanoscale silicon step-index waveguides: a general framework of selection rules and calculating SBS gain," *Optics Express*, vol. 21, no. 25 , 2013.
- [20] B.D.Hauer, C.Doolin, K.S.D. Beach and J.P.Davis, "A general procedure for thermomechanical calibration of nano/micro-mechanical resonators," *arXiv:1305.0557*.
- [21] G.Bahl, M.Tomes, F.Marquardt and T.Carmon, "Observation of spontaneous Brillouin cooling," *Nature Physics*, vol. 8, 2012.